

Endoglin Null Endothelial Cells Proliferate Faster and Are More Responsive to Transforming Growth Factor β 1 with Higher Affinity Receptors and an Activated Alk1 Pathway*

Received for publication, March 30, 2005, and in revised form, May 23, 2005
Published, JBC Papers in Press, May 27, 2005, DOI 10.1074/jbc.M503471200

Nadia Pece-Barbara^{‡§}, Sonia Vera[¶], Kirishanthy Kathirkamathamby^{||}, Stefan Liebner^{**},
Gianni M. Di Guglielmo[‡], Elisabetta Dejana^{**}, Jeffrey L. Wrana^{‡‡}, and Michelle Letarte^{||§§}

From the [‡]Programme in Molecular Biology and Cancer, Samuel Lunenfeld Research Institute, Mount Sinai Hospital, the [¶]Cancer Research Program, Hospital for Sick Children, and the ^{||}Heart and Stroke Lewar Center of Excellence and Department of Immunology, University of Toronto, Ontario M5G 1X8, Canada and ^{**}Italian Foundation for Cancer Research Institute of Molecular Oncology and Department of Biomolecular and Biotechnological Sciences, University of Milan, Milan 20146, Italy

Endoglin is an accessory receptor for transforming growth factor β (TGF β) in endothelial cells, essential for vascular development. Its pivotal role in angiogenesis is underscored in Endoglin null (*Eng*^{-/-}) murine embryos, which die at mid-gestation (E10.5) from impaired yolk sac vessel formation. Moreover, mutations in endoglin and the endothelial-specific TGF β type I receptor, ALK1, are linked to hereditary hemorrhagic telangiectasia. To determine the role of endoglin in TGF β pathways, we derived murine endothelial cell lines from *Eng*^{+/+} and *Eng*^{-/-} embryos (E9.0). Whereas *Eng*^{+/+} cells were only partially growth inhibited by TGF β , *Eng*^{-/-} cells displayed a potent anti-proliferative response. TGF β -dependent Smad2 phosphorylation and Smad2/3 translocation were unchanged in the *Eng*^{-/-} cells. In contrast, TGF β treatment led to a more rapid activation of the Smad1/5 pathway in *Eng* null cells that was apparent at lower TGF β concentrations. Enhanced activity of the Smad1 pathway in *Eng*^{-/-} cells was reflected in higher expression of ALK1-dependent genes such as *Id1*, *Smad6*, and *Smad7*. Analysis of cell surface receptors revealed that the TGF β type I receptor, ALK5, which is required for ALK1 function, was increased in *Eng*^{-/-} cells. TGF β receptor complexes were less numerous but displayed a higher binding affinity. These results suggest that endoglin modulates TGF β signaling in endothelial cells by regulating surface TGF β receptors and suppressing Smad1 activation. Thus an altered balance in TGF β receptors and downstream Smad pathways may underlie defects in vascular development and homeostasis.

Endoglin (CD105) is a homodimeric transmembrane glycoprotein expressed on all types of endothelial cells (1) and in-

creased in cells in culture and during angiogenesis *in vivo* (2–7). Endoglin expression is also enhanced in vascular smooth muscle cells during injury and inflammation (8–10). Endoglin is critically important in the cardiovascular system as revealed by a lethal phenotype in endoglin null (*Eng*^{-/-}) murine embryos at gestational day E10.5 because of defects in vessel and heart development (11–13). Vasculogenesis in the *Eng*^{-/-} mice is normal, but angiogenesis is impaired along with remodeling of the primary vascular plexus. Mice exhibit poor vascular smooth muscle development that results in dilatation and rupture of the vascular channels. Heart development is arrested in *Eng*^{-/-} mice at E9.0. The atrioventricular canal endocardium fails to undergo mesenchymal transformation and to generate the cushion tissue essential for valve formation and heart septation (11). Transient expression of endoglin is also striking during human development, as it is up-regulated during heart valve formation but subsequently reduced as the valves mature (14). In the adult vasculature, endoglin haploinsufficiency causes the vascular dysplasia hereditary hemorrhagic telangiectasia type 1 (HHT1)¹ associated with dilated vessels and arteriovenous malformations (15, 16).

Endoglin associates with transforming growth factor β (TGF β) receptors (17). TGF β is a multifunctional cytokine that controls proliferation, migration, adhesion, and apoptosis of diverse cell types (18, 19). TGF β signals through a heteromeric complex of type I and type II transmembrane serine/threonine kinase receptors (20). Receptor activation occurs upon binding of ligand to the type II receptor (T β R_{II}), which recruits and phosphorylates type I receptors and then propagates the signal to downstream target receptor-regulated Smads (21, 22). The specificity of cellular responses to TGF β is mediated by the type I receptors. Most cells utilize the type I receptor ALK5, which phosphorylates Smad2 and Smad3. However, endothelial cells have an additional type I receptor, ALK1, which phosphorylates Smad1 and Smad 5 (23, 24). Of note, TGF β -dependent activation of ALK1 requires ALK5, such that both are present with T β R_{II} in a composite receptor complex that acts via Smad1 and Smad5. Once phosphorylated, one of these receptor-regulated Smads combines with the common Smad4,

* This work was supported in part by grants from the Canadian Institute of Health Research (to J. L. W. and M. L.), the Heart and Stroke Foundation of Canada (to M. L.), and the National Cancer Institute of Canada (to J. L. W.). The costs of publication of this article were defrayed in part by the payment of page charges. This article must therefore be hereby marked "advertisement" in accordance with 18 U.S.C. Section 1734 solely to indicate this fact.

§ Recipient of a postdoctoral fellowship from the Canadian Digestive Disease Foundation/Canadian Institutes of Health Research.

‡‡ An International Scholar of the Howard Hughes Medical Institute.

§§ To whom correspondence should be addressed: Cancer Research Program, Hospital for Sick Children, 555 University Ave., Toronto, Ontario M5G 1X8, Canada. Tel.: 416-813-6258; Fax: 416-813-6255; E-mail: mabl@lab@sickkids.ca.

¹ The abbreviations used are: HHT, hereditary hemorrhagic telangiectasia; TGF β , transforming growth factor β ; *ENG*, endoglin gene; E3, ubiquitin-protein isopeptide ligase; MEEC, murine embryonic endothelial cells; T β R_{II}, TGF β type II receptor; ALK, activin receptor-like kinase; *ACVRL1*, activin receptor-like kinase 1 gene; FBS, fetal bovine serum; pAb, polyclonal antibody; mAb, monoclonal antibody; FITC, fluorescein isothiocyanate; PECAM, platelet/endothelial cell adhesion molecule.

and the complex translocates to the nucleus to regulate transcription (22, 25). The inhibitory Smads 6 and 7 are a third class of Smads that down-regulate TGF β -related responses (26) primarily through recruitment of E3 ligases to active receptor complexes, leading to ubiquitin-mediated degradation by the 26 S proteasome (27, 28).

TGF β 1 has various roles in development and homeostasis of the vascular system and regulates both vasculogenesis and angiogenesis. It can regulate vascular permeability, endothelial cell proliferation and migration, production of extracellular matrix, and vascular remodeling (29). Recruitment of mesenchymal cells into new vessels is achieved in part by TGF β . Upon contact of mesenchymal cells with the endothelium, latent TGF β is activated, inducing differentiation of mesenchymal cells into pericytes and smooth muscle cells (30). Gene ablation of TGF β , its receptors, and Smads underscores the essential role of TGF β signaling in vascular development. Gene knock-outs of TGF β 1, T β R2, ALK5, ALK1, and Smad5 all die from improper development of yolk sac vascular networks and/or cardiac malformations. Although T β R2 and ALK5 null mice also have yolk sac defects, the most similar phenotypes to endoglin null mice are the ALK1- and Smad5-deficient embryos, which also develop dilated vessels ascribed to poor smooth muscle cell development (31). Moreover, mutations in the *ACVRL1* gene, which codes for ALK1, cause HHT2, exhibiting vascular lesions similar to HHT1, suggesting that endoglin and ALK1 may function in the same pathway (32).

Endoglin does not bind TGF β on its own but associates with TGF β receptor complexes primarily by interacting with the ligand binding receptor T β R2 (17). Endoglin also interacts with ALK5 and ALK1 in the absence of TGF β (33, 34). Although endoglin is thought to modulate TGF β signaling, its role in the endothelial cell receptor complex is not well understood. Ectopic overexpression of endoglin in myoblasts and activated monocytes interferes with several TGF β responses, including inhibition of proliferation (35, 36). Similarly, treatment of endothelial cells with antisense oligonucleotides for endoglin enhanced the ability of TGF β 1 to suppress growth and migration of these cells (37).

To better understand the role of endoglin in the vascular system, we analyzed TGF β signaling in *Eng*^{-/-} and control murine embryonic endothelial cells (MEEC). Our results are consistent with a model in which endoglin modulates TGF β -dependent activation of ALK1 versus ALK5 to maintain a balance between Smad1/5 and Smad2/3 signaling pathways in endothelial cells.

EXPERIMENTAL PROCEDURES

Derivation of MEEC—*Eng*^{+/+} and *Eng*^{-/-} murine embryos and yolk sacs were isolated at E9.0 of gestation (N4 generation, C57BL/6 mice), prior to onset of the lethal phenotype in the *Eng* null mice as previously described (38). After disaggregation of tissues, endothelial cells were selectively immortalized with polyoma middle T antigen in the retrovirus vector N-TkMT using 8 μ g/ml polybrene (Sigma), and lines were established as reported (38). The infected cells were selected by adding the neomycin analogue G418 (Invitrogen) at 800 μ g/ml. Cells were maintained in MCDB131 medium plus 15% fetal bovine serum (FBS) and 15 μ g/ml endothelial mitogen (Biomedical Technologies), heparin 10 units/ml (Hepalean), gentamicin 50 μ g/ml (Wisent), and glutamine 1% (Amersham Biosciences).

Two-color Flow Cytometry—MEEC were detached by brief trypsinization, neutralized with 15% FBS, and washed in Ca²⁺-Mg²⁺-free phosphate-buffered saline plus 2% FBS. Cells (1 \times 10⁶) were incubated for 1 h with saturating amounts of FITC-conjugated monoclonal antibody (mAb) MJ7/18 (Biocan Scientific) to murine endoglin (CD105), phosphatidylethanolamine-conjugated mAb MEC 13.3 to PECAM (CD31; BD Biosciences) or respective conjugated isotype controls and then washed again. Samples were run on the fluorescence-activated cell sorter Calibur[®] (BD Biosciences). A gate was set using forward and side scatter and both FL1 (FITC) and FL2 (phosphati-

dylethanolamine) channels were acquired. Data were analyzed using CellQuest[®] software where percent positive cells were determined relative to the isotype controls.

Metabolic Labeling and Immunoprecipitation—Equivalent numbers of matched MEEC lines were incubated with 100 μ Ci/ml [³⁵S]methionine (Tran³⁵S-label; ICN Pharmaceuticals) in methionine-free Dulbecco's modified Eagle's medium for 3.5 h. Cells were solubilized in lysis solution containing 1% Triton X-100 (Sigma) and a mixture of inhibitors, immunoprecipitated with mAb MJ7/18 (Biocan Scientific) to endoglin, and processed according to published procedures (16).

Determination of Proliferation Rates—To measure doubling time of MEEC, they were seeded at 1 \times 10⁵ (100-mm dish) in complete medium containing 15% FBS. At successive times post-seeding, cells were trypsinized, neutralized with 15% FBS, washed in phosphate-buffered saline, and counted in a Coulter counter (Beckman Coulter). The proliferation rate of lines was measured by [³H]thymidine incorporation. Cells were seeded at 2,000 cells/well (96-well plate) in complete medium containing 1% FBS and 15 μ g/ml endothelial mitogen (Biomedical Technologies) and then pulsed for 8 h (1 μ Ci/well) at various time points. Cells were lysed with water and harvested with a microplate harvester (Inotech Biosystems International); radioactive incorporation was determined by liquid scintillation analysis (Beckman Instruments). Multiple conditions were tested for cell density, growth factor, FBS concentrations, and length of pulse. Results reported here show an optimal experiment with reduced serum. For inhibition of proliferation by TGF β 1 (R&D Systems), cells were left overnight in complete medium containing 15% FBS and 15 μ g/ml endothelial mitogen, starved for 2 h, and incubated with increasing concentrations of TGF β 1 ranging from 0 to 100 pM in medium containing 1% FBS and 15 μ g/ml endothelial mitogen for 48 h, including an 8-h pulse with [³H]thymidine (1 μ Ci/well). These conditions were optimized for cell density, growth factor concentration, and time in culture with both matched sets of lines to obtain maximal inhibition of proliferation by TGF β 1.

Measurement of Smad Phosphorylation by Western Blot—Equivalent numbers of MEEC were seeded in complete medium. After 48 h, cells were starved for 2–3 h in serum-free medium, treated with TGF β 1 for the times and concentrations indicated, and solubilized in lysis solution containing 1% Triton X-100 and a mixture of inhibitors (20). Protein concentration was estimated, and volumes of samples with equivalent protein were fractionated by 8% SDS-PAGE and electrotransferred to nitrocellulose. Blots were immunoprobed, processed, and detected as reported (16) except that chemiluminescence detection was performed using SuperSignal West Dura (Pierce) and blots quantified using a Fluor-S-max[®] CCD camera and QuantityOne software (Bio-Rad) or exposed to Hyper-film (Amersham Biosciences) and films scanned by densitometer. Antibodies used for detection were polyclonal antibody (pAb) to phospho-Smad2 (Cell Signaling), mAb to Smad2/3 (Transduction Laboratories), pAb to phospho-Smad1/5/8 (Cell Signaling), pAb to Smad1/5 prepared in-house (Wrana) or from Cell Signaling. Anti- β -actin (Sigma) was used to reprobe blots to determine equal loading.

Smad2/3 Nuclear Translocation Assay—15,000 cells of each MEEC line were seeded per well of 96-well plates and after 24 h were rinsed, starved for 2 h in serum-free MCDB131 medium, and treated with TGF β 1 in medium containing 0.2% FBS for the times and concentrations indicated. Cells were fixed for 10 min by adding paraformaldehyde to a final concentration of 4% and permeabilized with 100% methanol for 2.5 min at 23 $^{\circ}$ C. After washing extensively, cells were blocked for 1 h with phosphate-buffered saline plus 10% FBS. Cells were incubated overnight at 4 $^{\circ}$ C with a mAb recognizing both Smad2 and Smad3 (Transduction Laboratories). They were washed and incubated with AlexaFluor 488-conjugated anti-mouse IgG (1:1000; Molecular Probes) plus 4',6-diamidino-2-phenylindole (DAPI) (1:2000; Sigma) to stain nuclei for 1 h at 23 $^{\circ}$ C. Nuclei were defined using the DAPI stain and fluorescence within a cytoplasmic ring, and the nucleus was measured with the FITC channel on the ArrayScanII[®] from Cellomics Instruments. The mean nuclear-cytoplasmic intensity difference was simultaneously quantified using the Molecular Translocation BioApplication[®] and Data Viewer software (Cellomics).

Real-time PCR of mRNA Levels—RNA was extracted by adding TRIzol (Invitrogen) directly onto washed MEEC monolayers. RNA quality and concentration were estimated using the Agilent Analyser. Samples were reverse transcribed into cDNA using oligo(dT) primers (Superscript II RT-PCR kit; Invitrogen) and the cDNA samples used in real-time PCR experiments. Glyceraldehyde-3-phosphate dehydrogenase was used as the housekeeping gene, and gene expression was measured using SYBR green II (Qiagen) with the ABI PRISM 7900 real-time PCR system. The primer sequences were obtained from Dr. Koichi Mishima (Dept. of Pathology, University of Tokyo, Tokyo). The

PCR program consisted of the initial activation step at 95 °C for 15 min, followed by 50 cycling steps of denaturing for 15 s at 94 °C, annealing at appropriate temperature for 30 s, and extension at 72 °C for 15 s. The PCR data were analyzed using SDS 2.1 software (Applied Biosystems).

Cell Surface Biotinylation and Western Blot—Receptor levels were quantified by Western blot analysis as described for Smad phosphorylation except that cells were not treated with TGF β 1. Antibodies used for detection were pAb C16 to T β RII (Santa Cruz Biotechnology), mAb MJ7/18 (Biocan Scientific) to murine endoglin, mAb to ALK1 (R&D systems), and pAb V22 to ALK5 (Santa Cruz). For quantification of cell surface T β RII, equivalent numbers of MEEC were seeded in complete medium; after 48 h, intact monolayers were surface labeled with 0.3 mg/ml of sulfo-succinimidyl 6 (biotinamido)-hexanoate (NHS-LC-Biotin; Pierce) as reported previously (16). Lysates from surface-biotinylated cells were immunoprecipitated with anti-T β RII pAb C16 (Santa Cruz) or anti-endoglin mAb MJ7/18 (Biocan Scientific). Samples containing equivalent protein content were analyzed by 4–12% SDS-PAGE (Novex) and probed with streptavidin-horseradish peroxidase as reported. Quantification was achieved by chemiluminescence with ECL (Amersham Biosciences) followed by reading with a Fluor-S-Max[®] CCD camera and QuantityOne software (Bio-Rad).

Affinity Labeling of Receptor Complexes, Turnover, and Scatchard Analysis—TGF β (R&D Systems) was iodinated with ¹²⁵I using chloramine-T as described previously (39). For turnover of active complexes, confluent monolayers were affinity labeled by incubation with 250 pM ¹²⁵I-TGF β 1 for 2 h at 4 °C, washed, and treated with disuccinimidyl suberate (Pierce). Cells were washed with phosphate-buffered saline-Tris (pH 7.6) and incubated in medium at 37 °C for the times indicated for receptor turnover experiments. Cells were then solubilized in lysis solution containing 1% Triton X-100 and a mixture of inhibitors as reported (40) and analyzed by SDS-PAGE on 4–12% gels (Novex). Receptors were quantified using a STORM Phosphorimager and ImageQuant software (Amersham Biosciences). For Scatchard analysis, confluent monolayers were incubated with increasing concentrations of ¹²⁵I-TGF β 1 in the presence or absence of 40 \times competing cold TGF β 1 at 4 °C for 3.5 h and cross-linked as described above. Labeling medium and supernatants were collected and counted in a gamma counter. Lysates were also counted and then analyzed by 4–12% SDS-PAGE (Novex). Pixels were converted to cpm by comparing to known amounts of ¹²⁵I-TGF β 1 that were spotted onto filters and exposed along with gels and quantified as above.

RESULTS

Eng Null Endothelial Cells Show Increased Proliferation and Growth Inhibitory Response to TGF β —To better understand the role of endoglin in TGF β -mediated signaling in endothelial cells, we generated endothelial cell lines from murine embryos and yolk sacs (E9.0) prior to onset of the lethal phenotype in *Eng* null mice as described under “Experimental Procedures.” *Eng*^{+/+} and *Eng*^{-/-} embryos from two founding mothers, numbered herein as 150 and 152, were independently used for the derivation of lines. When embryonic cells are infected with retrovirus vectors containing polyoma middle T antigen, endothelial cells are selectively immortalized. This allows pure wild type and endoglin null MEEC lines to be obtained even if starting from a mixed population. Fig. 1A shows the characterization of these lines: *Eng*^{+/+} 150/7 with *Eng*^{-/-} 150/9 and *Eng*^{+/+} 152/8 with *Eng*^{-/-} 152/10. Two-color flow cytometry analysis revealed that 96–98% of *Eng*^{+/+} cells were in the upper right quadrant and thus were positive for endoglin (CD105) and PECAM (CD31). Alternatively, 90–93% of *Eng*^{-/-} cells were in the upper left quadrant and thus were positive for the endothelial cell marker PECAM, indicating that these MEEC lines were endothelial but lacked endoglin. Analysis of endoglin expression by metabolic labeling followed by SDS-PAGE (Fig. 1B) demonstrated that wild type cells expressed the full-length monomeric glycosylated (*E*) and precursor (*P*) forms, whereas no endoglin was detectable in the mutants.

Next we analyzed the proliferation rate of the *Eng*^{-/-} and control *Eng*^{+/+} MEEC lines and found that *Eng*^{-/-} cells proliferated faster and achieved higher cell densities when compared with wild type cells (Fig. 2, A and B). Subsequently, we examined TGF β -dependent inhibition of proliferation. Although TGF β is a potent inhibitor of proliferation in epithelial cells,

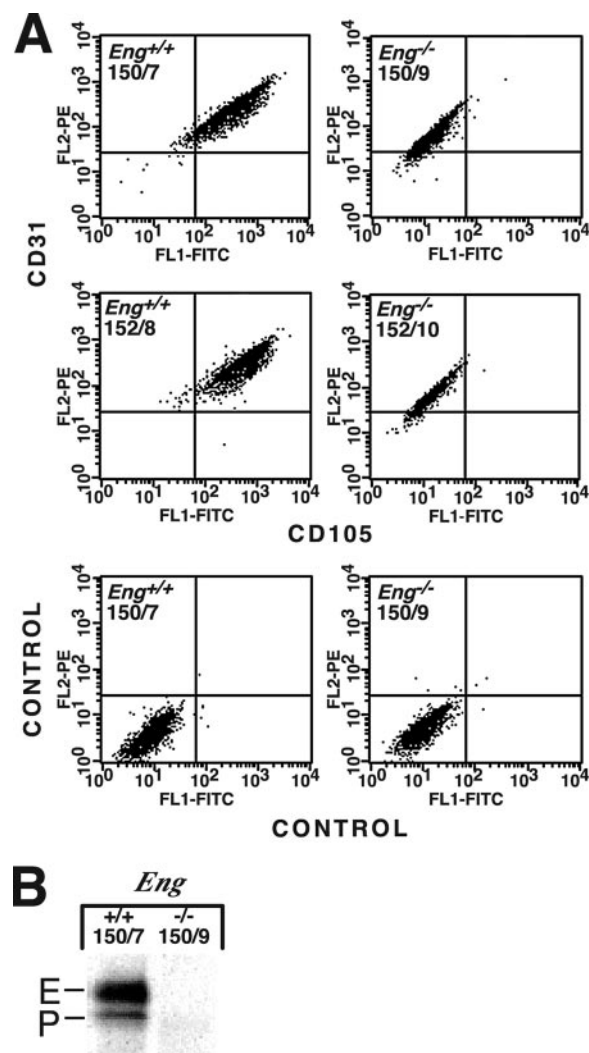


FIG. 1. Characterization of embryonic endothelial cells derived from *Eng*^{+/+} and *Eng*^{-/-} mice. A, two-color flow-cytometry analysis of endoglin (CD105) and PECAM (CD31) expressed on mouse embryonic endothelial cell lines using a FITC-conjugated anti-CD105 and a phosphatidylethanolamine-conjugated anti-CD31. A representative experiment is shown for two sets of matched MEEC lines, *Eng*^{+/+} 150/7 with *Eng*^{-/-} 150/9 and *Eng*^{+/+} 152/8 with *Eng*^{-/-} 152/10. 96–98% of *Eng*^{+/+} cells were in the upper right quadrant, whereas 90–93% of *Eng*^{-/-} cells were in the upper left quadrant. Markers for each axis were set with FITC-conjugated and phosphatidylethanolamine-conjugated isotype-matched control antibodies shown in lower panels with 99% negative cells in the lower left quadrant. B, endoglin expression was analyzed by metabolic labeling with [³⁵S]methionine and solubilization in Triton X-100. Lysates containing equivalent cpm were immunoprecipitated with anti-CD105 and fractionated using SDS-PAGE under reducing conditions. Monomeric glycosylated endoglin (*E*) and precursor (*P*) are observed only in *Eng*^{+/+} lysates.

both wild type endothelial cell lines examined here displayed poor responses (Fig. 2C), similar to previously published reports in other endothelial cell types (16, 41, 42). In contrast, when we examined the *Eng*^{-/-} lines, we observed potent anti-proliferative responses to TGF β , with over 80% inhibition observed at between 25–50 pM (Fig. 2C). Of note, none of our cell lines displayed a TGF β -dependent proliferative response, contrasting with MEEC cells reported by Lebrin *et al.* (7) that displayed a “low-dose” TGF β -induced proliferation dependent on endoglin. Our data suggest that in wild type cells, endoglin functions to block TGF β -dependent inhibition of proliferation, in agreement with published data of a knockdown of endoglin in endothelial cells using antisense oligonucleotides leading to enhanced growth inhibition by TGF β 1 (37).

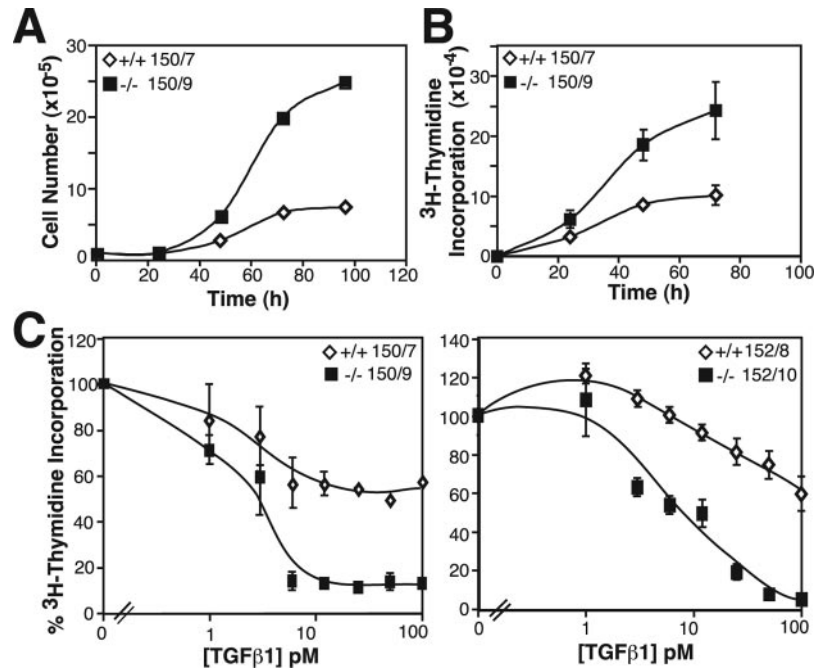


FIG. 2. Proliferation rate of $Eng^{+/+}$ and $Eng^{-/-}$ MEEC lines. A, doubling time of MEEC lines. $Eng^{+/+}$ 150/7 (◇) and $Eng^{-/-}$ 150/9 (■) were seeded at 1×10^5 cells/dish in complete medium with 15% FBS. At the indicated times, cells were trypsinized and counted in a Coulter counter. B, proliferation rate of lines $Eng^{+/+}$ 150/7 (◇) and $Eng^{-/-}$ 150/9 (■) was measured by [³H]thymidine incorporation. Cells were seeded at 2,000 cells/well in complete medium with 1% FBS and pulsed for 8 h at various time points. Total incorporation (cpm) is plotted versus total time including the pulse ($n = 3$ for each time point). C, inhibition of proliferation by TGFβ of $Eng^{-/-}$ MEEC lines (■) relative to normal (◇). Cells were seeded at 2,000 cells/well and incubated with increasing concentrations of TGFβ1 for 24 h. An 8-h pulse with [³H]thymidine was performed, and the percent incorporation relative to control (no TGFβ1) was calculated for each concentration. The mean of two experiments for 150/7 and 150/9 is illustrated, whereas a representative experiment is shown for 152/8 and 152/10 ($n = 6$ for each time point). Error bars represent the mean \pm S.D.

Endoglin Does Not Alter TGFβ1 Activation of Smad2 in MEEC Lines—To better define a mechanism for the increased TGFβ responsiveness in the $Eng^{-/-}$ lines, we looked at downstream signaling events, namely Smad2 phosphorylation and nuclear accumulation (Fig. 3). We first examined Smad2 phosphorylation in response to increasing doses of TGFβ using a phospho-specific antibody that recognizes activated Smad2. This revealed robust Smad2 activation that was near maximal at 5 pM, the lowest dose of TGFβ1 tested (Fig. 3A). Next we examined the rate of Smad2 activation in response to 50 pM TGFβ1 and observed that, whereas $Eng^{-/-}$ cells displayed a slightly earlier activation of Smad2 (Fig. 3B), there was no difference when we assessed the magnitude and endurance of Smad2 activation in response to a brief 30-min pulse of TGFβ1 (Fig. 3C). We also quantified the nuclear accumulation of Smad2 and Smad3 in the nucleus using a Cellomics Arrayscan system (28, 43). Consistent with our analysis of Smad2 phosphorylation, we observed no difference in the magnitude or the kinetics of TGFβ-dependent Smad2/3 nuclear accumulation when comparing $Eng^{+/+}$ to $Eng^{-/-}$ cells (Fig. 3D).

$Eng^{-/-}$ Cells Have an Activated ALK1 Pathway—In endothelial cells, TGFβ has been shown to activate Smad1 via ALK1. Because ALK5 kinase activity is needed for ALK1 signaling, both type I receptors assemble in a heteromeric receptor complex that activates the Smad1/5/8 pathway. Therefore, we next tested TGFβ-dependent activation of the Smad1/5/8 pathway using an antibody that recognizes phospho-Smad1, Smad5, and Smad8 (Fig. 4).

In contrast to the Smad2/3 pathway, analysis of the dose response of Smad1/5/8 activation after 15 min of stimulation revealed a robust response in the 150/9 $Eng^{-/-}$ cells, even at the lowest doses of TGFβ1 tested. Strikingly, there was little or no induction at low doses in the matched $Eng^{+/+}$ MEECs (Fig. 4A). Furthermore, we consistently observed enhanced basal

levels of phospho-Smad1/5/8 in these cells that may be due to some low level of autocrine signaling. We then examined temporal kinetics in these cells using a high dose of TGFβ1 and found a more rapid activation of Smad1/5/8 in the 150/9 $Eng^{-/-}$ cells (Fig. 4B) that was evident within 5 min of stimulation and was quite pronounced when the cells were subjected to a brief pulse with TGFβ1 (Fig. 4C). Similar results were obtained when we analyzed the 152/8 and 152/10 matched set of $Eng^{+/+}$ and $Eng^{-/-}$ cells (data not shown). Our analysis of the Smad1 pathway suggests that it is basally active and highly responsive in the mutant lines. Therefore, we measured the expression of Smad6, Smad7, and Id1, which were shown to be specifically up-regulated by constitutive ALK1 activity in endothelial cells (44), using real-time quantitative PCR (Fig. 4D). Consistent with Smad1 pathway activation, we found that when compared with wild type cells, $Eng^{-/-}$ cells displayed elevated levels of Smad6 (10-fold), Smad7 (4.5-fold), and Id1 (2–2.5-fold), whereas Smad1, Smad2, and plasminogen activator inhibitor (PAI-1), a TGFβ target gene, were unchanged (Fig. 4D). Our data suggest that loss of Eng has little impact on the Smad2/3 pathway but leads to up-regulation of the Smad1 pathway that is likely due to enhanced signaling through ALK1, which specifically regulates Smad1/5/8 (45). Of particular note, we also analyzed TGFβ induction of Smad-independent pathways such as mitogen-activated protein kinase by measuring phosphorylation of p44/p42 as well as p38 and found that these pathways were not strongly regulated by TGFβ in these cells (data not shown).

Eng Null MEEC Display Reduced Numbers of Cell Surface TGFβ Receptors but Increased Binding Affinity—Signaling by TGFβ is initiated by binding to TβRII followed by recruitment of ALK5 or ALK5-ALK1 complexes in endothelial cells. Because loss of Eng leads to enhanced activation of the Smad1/5/8 pathway, we therefore examined the TGFβ receptor complement in

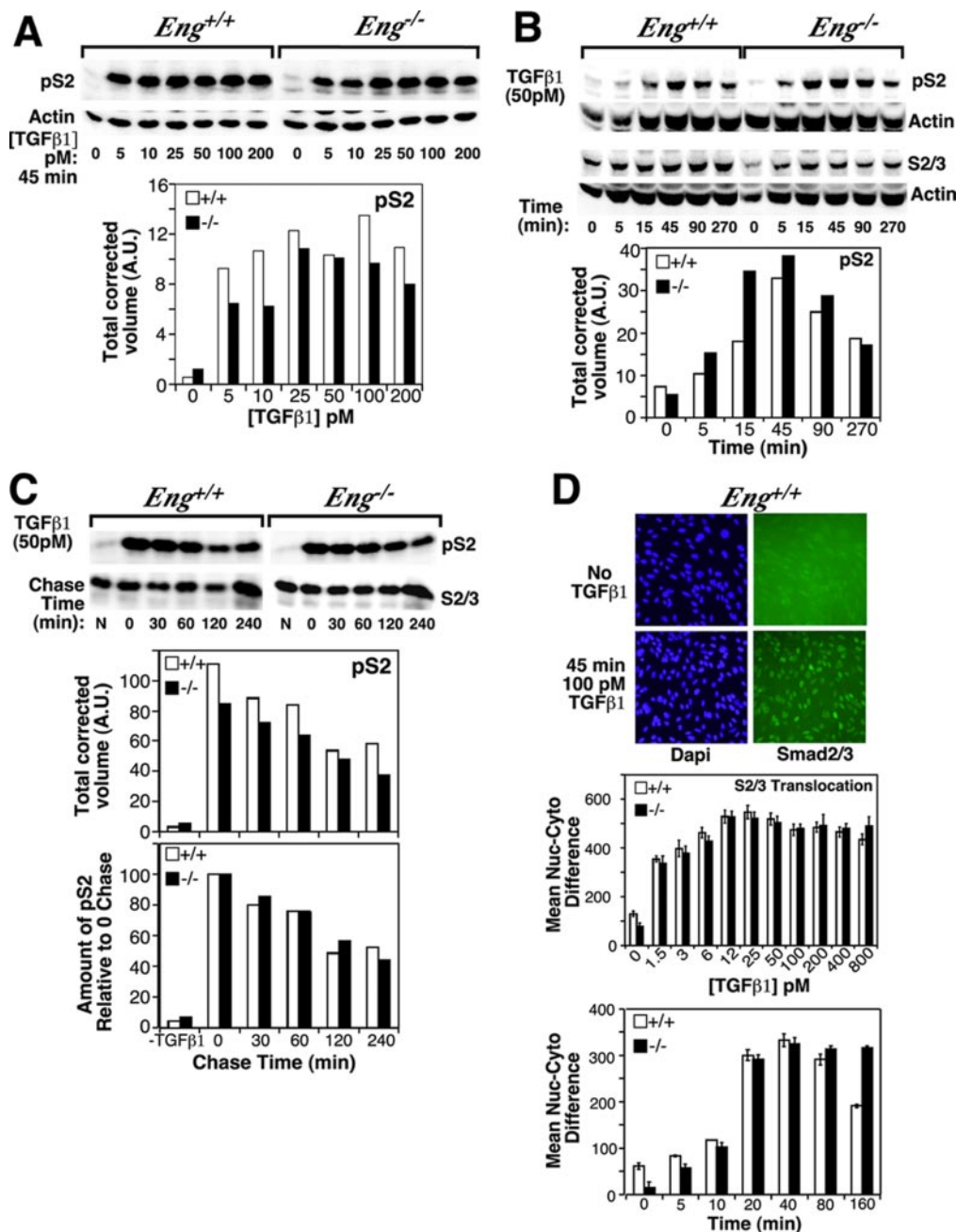


FIG. 3. Smad2 phosphorylation and Smad2/3 translocation in MEEC lines. *A*, $Eng^{+/+}$ or $Eng^{-/-}$ cells were starved for 2–3 h in serum-free medium and stimulated for 45 min with TGF β 1 at the indicated dose. Equal volumes of lysates containing equivalent protein were analyzed by SDS-PAGE and Western blot with the indicated antibodies. The amount of phosphorylated Smad2 (pS2) was quantified by chemiluminescence, and the volume corrected for background was plotted in arbitrary units (A.U.). Total β -actin as a loading control was also probed and quantified, revealing no significant difference in loading. *B*, $Eng^{+/+}$ and $Eng^{-/-}$ cells were starved for 2–3 h in serum-free medium and stimulated with 50 pM TGF β 1 for the indicated times. Equal volumes of lysates containing equivalent protein were fractionated by SDS-PAGE and analyzed as in panel A. Total Smad2/3 (S2/3) levels along with β -actin were also probed. Quantification of S2/3 with β -actin demonstrated no significant difference in S2/3 levels (not shown). *C*, $Eng^{+/+}$ and $Eng^{-/-}$ cells were starved for 2–3 h in serum-free medium, treated with 50 pM TGF β 1 for 30 min, and then chased with medium containing 0.2% FBS for the times shown. Samples were analyzed as in panel A. Both raw data showing the total volume of the pSmad2 (pS2) band corrected for background (upper graph) and the amount of pS2 relative to the 0 chase time (30-min pulse) were plotted (lower graph). N represents no TGF β 1 in the Western blot panels. Only raw data are plotted on both graphs for this negative control. Total Smad2/3 (S2/3) levels were also probed. Quantification of S2/3 demonstrated no significant difference in S2/3 levels (not shown). *D*, 15,000 cells of each $Eng^{+/+}$ and $Eng^{-/-}$ were seeded per well onto 96-well plates and after 24 h were rinsed, starved for 2 h in serum-free medium, and incubated with the serial dilutions of TGF β 1 for 45 min. Cells were fixed, permeabilized, and stained with anti-Smad2/3 mAb followed by an Alexafluor 488-conjugated anti-IgG and the 4',6-diamidino-2-phenylindole nuclear stain. Translocation was measured using an ArrayScan $\text{\textcircled{R}}$ and the Molecular Translocation BioApplication $\text{\textcircled{R}}$ (Cellomics). Upper panels show images of $Eng^{+/+}$ cells treated for 45 min with or without TGF β 1. Similar images were obtained with $Eng^{-/-}$ cells, not shown. The mean nuclear-cytoplasmic difference indicating Smad2/3 translocation levels was plotted at different TGF β 1 concentrations (upper graph) or at different times with 50 pM TGF β 1 (lower graph). Representative assays of three independent experiments are shown. Error bars represent the mean \pm S.D. with $n = 4$ for each point.

MEEC. Analysis of receptor mRNA levels revealed no difference in ALK1 or T β RII; however, ALK5 levels were elevated 2–2.5-fold in the endoglin null MEEC relative to control (Fig. 5A). Western

blot analysis further showed that ALK5 protein was elevated in the endoglin null cells, whereas T β RII protein was somewhat reduced in both endoglin null lines compared with normal, and

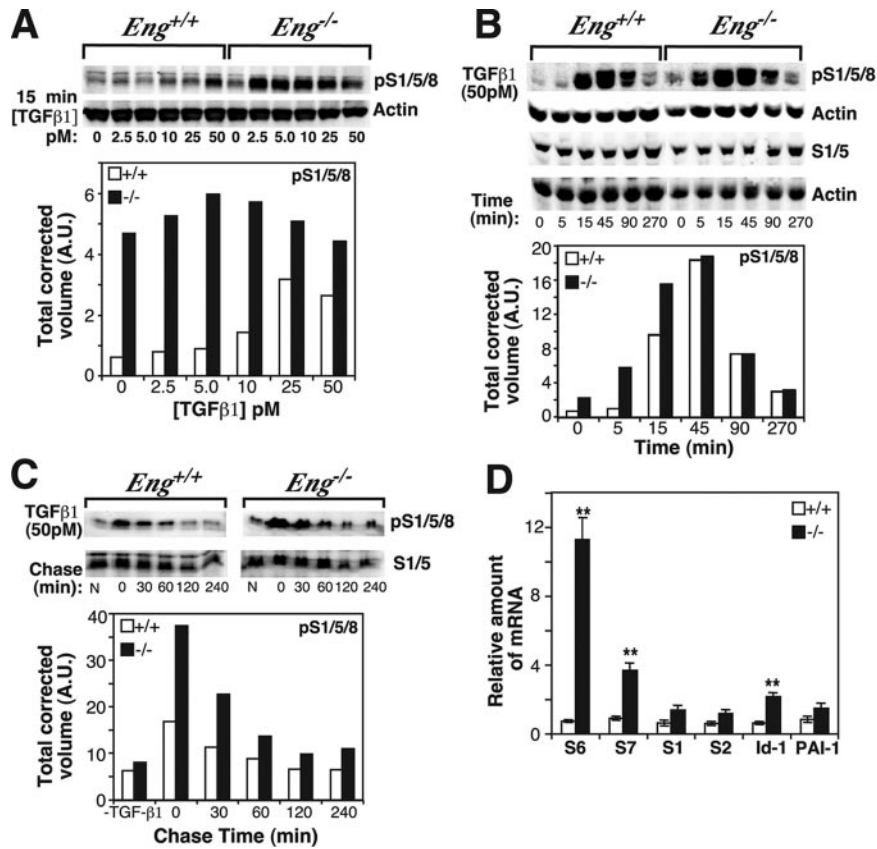


FIG. 4. Smad1/5/8 phosphorylation is increased in *Eng*^{-/-} MEEC lines. *A*, cells were starved for 2–3 h in serum-free medium and stimulated for 15 min with TGFβ1 at the indicated doses. Equal volumes of lysates containing equivalent protein were analyzed by SDS-PAGE and Western blot. The amount of phosphorylated Smad1/5 (*pS1/5/8*) was quantified by densitometry scan; the volume was corrected for background and plotted in arbitrary units (A.U.). Quantification of β-actin levels showed no significant difference in the loading (not shown). Total Smad1/5 (*S1/5*) levels along with β-actin as loading controls for each were also probed and quantified; however, the *S1/5* levels remained constant (not shown). *B*, MEEC lines *Eng*^{+/+} 150/7 and *Eng*^{-/-} 150/9 were starved for 2–3 h in serum-free medium and then stimulated with 50 pM TGFβ1 for the indicated times. Samples were analyzed as in *panel A*. Total Smad1/5 (*S1/5*) levels along with β-actin were also probed, and their quantification demonstrated no significant difference in levels (not shown). *C*, *Eng*^{+/+} and *Eng*^{-/-} MEEC lines 150/7 and 150/9 were starved for 2–3 h in serum-free medium, treated with 50 pM TGFβ1 for 30 min, and then chased with medium containing 0.2% FBS for the times shown. Samples were analyzed as in *panel A*. The raw data showing the total volume of the *pSmad1/5/8* band corrected for background were plotted. *N* represents no TGFβ1 in the Western blot panels. *D*, the levels of Smad6 (*S6*), Smad7 (*S7*), Smad1 (*S1*), inhibitor of differentiation (*Id-1*), and plasminogen activator inhibitor (*PAI-1*) mRNA in *Eng*^{+/+} line 150/7 versus control *Eng*^{-/-} line 150/9 for *S6* and *S7* ($n = 9$) and for *S1*, *Id-1*, and *PAI-1* ($n = 6$) were measured by real-time PCR. The relative amounts of these mRNA were obtained by normalization to glyceraldehyde-3-phosphate dehydrogenase levels. Error bars represent mean ± S.D. Genes showing a statistical difference between the two groups ($p < 0.001$) are marked by **.

ALK1 levels were similar in all the lines (Fig. 5B). Quantitation of protein levels from several experiments showed that ALK5 protein in the mutants was elevated by 2.2-fold and TβRII protein reduced to 70% of control levels. Furthermore, we examined cell surface TβRII using surface biotinylation of all four matched MEEC lines followed by immunoprecipitation with anti-TβRII and detection using streptavidin. This revealed that *Eng*^{-/-} cells have ~60% of TβRII compared with *Eng*^{+/+} cells, similar to the overall 70% reduction observed by Western blot (Fig. 5C). Analysis with anti-endoglin as a control for the same samples confirmed no surface endoglin on the null cells. Because binding of TGFβ to TβRII is required for the assembly of functional heteromeric receptor complexes, we next examined TGFβ binding kinetics to both TβRII and type I receptors on MEEC by Scatchard analysis. As ALK1 co-migrates with ALK5, we could not distinguish between these two receptors. However, previous data have shown that ALK1 binds TGFβ in these cells in a complex with ALK5, so it is reasonable to assume that the affinity and cell surface numbers reflect the binding kinetics of both ALK5 and ALK1. Fig. 5D shows a representative experiment using *Eng*^{+/+} 152/8 and *Eng*^{-/-} 152/10 lines, and Table I gives a summary of the data obtained with these lines. From the Scatchard analysis, we found that the K_D of both TβRII and the type I receptors were 2.5–4-fold lower in the *Eng*^{-/-} lines, indicating higher affinity

binding complexes, whereas the number of sites per cell was reduced by 4–7-fold for both receptors. Although we cannot determine from this data which type I receptor is affected or if there is a shift in binding preferentially to ALK1, it is apparent that in MEEC endoglin expression leads to a larger number of lower affinity receptor complexes. This is the first report providing evidence that endogenous endoglin modulates the affinity and number of TGFβ receptor complexes in endothelial cells. Furthermore, because ALK5 is required for ALK1 activity (46), the increased numbers of ALK5 coupled to the enhanced affinity displayed by TGFβ receptors in *Eng*^{-/-} MEEC may enhance activation of the Smad1 pathway. Altogether, our results suggest that endoglin alters the balance of Smad2/3 versus Smad1/5/8 activation through regulation of endothelial cell surface TGFβ receptor complexes.

DISCUSSION

In the mouse embryo, endoglin is essential for angiogenesis. Endoglin has been previously described as a marker of proliferating endothelial cells, as its expression is up-regulated on cycling cells and during angiogenesis (2–7). However, it is not clear whether endoglin mediates an enhanced proliferative rate or may be up-regulated as part of a negative feedback loop. Our observation that *Eng*^{-/-} MEEC lines display a much

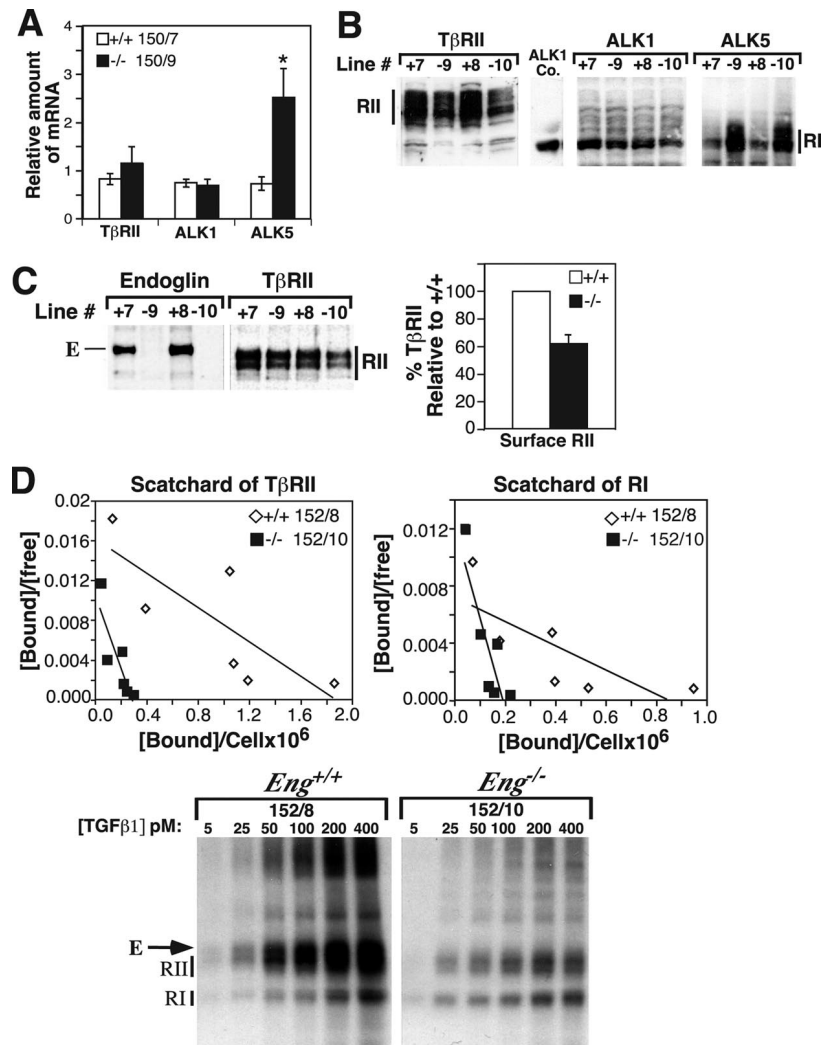


FIG. 5. ALK5 levels are increased and T β RII levels decreased in *Eng*^{-/-} MEEC leading to a lower number of higher affinity TGF β 1 binding sites. **A**, levels of T β RII (*RII*), ALK1, and ALK5 mRNA were measured by real-time PCR ($n = 9$ for *RII*, and $n = 6$ for ALK1 and ALK5). ALK5 marked by * shows a statistical difference between lines ($p < 0.05$). **B**, Western blot analysis of T β RII, ALK1, and ALK5 in both matched sets of MEEC lines *Eng*^{+/+} 150/7, *Eng*^{-/-} 150/9, *Eng*^{+/+} 152/8, *Eng*^{-/-} 152/10. Lysates containing equivalent total protein were analyzed by Western blot with pAb C16 to T β RII (*RII*), mAb to ALK1, and pAb to ALK5. The identification of ALK1 was confirmed using the ALK1 control (*Co.*) provided with the antibody. **C**, total surface T β RII (*RII*) was quantified by biotinylation of intact MEEC lines with sulfo-succinimidylyl 6 (biotinamido)hexonate. Lysates from surface-biotinylated cells were immunoprecipitated with anti-endoglin or anti-T β RII, and samples containing equivalent protein content were analyzed by SDS-PAGE, probed with streptavidin-horseradish peroxidase, and quantified by chemiluminescence. For total surface-labeled T β RII, the amount of receptor in the *Eng*^{-/-} MEEC lines is graphed relative to the total labeled in *Eng*^{+/+} lines from four experiments with an $n = 6$ (\pm S.D.). **D**, Scatchard analysis of TGF β receptor complexes in *Eng*^{+/+} and *Eng*^{-/-} MEEC lines. Confluent monolayers were affinity labeled with increasing concentrations of ¹²⁵I-TGF β 1 in the presence or absence of 40 \times competing cold TGF β 1 at 4 $^{\circ}$ C for 3.5 h. Supernatants were collected and counted. Lysates were analyzed by SDS-PAGE. The specific amount of ¹²⁵I-TGF β 1 bound to T β RII and type I receptors was quantified by Phosphorimager analysis and corrected with values from cold gels. Pixels were converted to cpm by spotting and quantifying aliquots of labeling medium. A representative experiment is shown along with its corresponding gels. The ratio bound/free was calculated and plotted *versus* the amount bound per cell, using the LINEST function of Excel, which draws the best-fit line using the least-squares method of regression analysis. The K_D for each line was estimated from the slope, and the x -axis intercept represents the number of sites/cell, summarized in Table I.

TABLE I

Summary of Scatchard analysis data of TGF β receptor complexes in *Eng* null and wild type MEEC lines

Confluent monolayers were affinity labeled with increasing concentrations of ¹²⁵I-TGF β 1 in the presence or absence of 40 \times competing cold TGF β 1 at 4 $^{\circ}$ C for 3.5 h. Supernatants were collected and counted. Lysates were analyzed by SDS-PAGE. The specific amount of ¹²⁵I-TGF β 1 bound to T β RII and type I receptors and the K_D and number of sites/cell for each receptor were quantified as described in Fig. 5D.

Cell line	Receptor II		Receptor I	
	K_D	No. of Sites/Cell	K_D	No. of Sites/Cell
<i>Eng</i> ^{+/+} 150/7	21 pM	1325	56 pM	1085
<i>Eng</i> ^{-/-} 150/9	5.7 pM	300	15 pM	150
<i>Eng</i> ^{+/+} 152/8	41 pM	1625	41 pM	770
<i>Eng</i> ^{-/-} 152/10	17 pM	270	8.7 pM	180

higher proliferative rate than control cells would be consistent with the latter model. This also correlates with our observation that the Smad1/5/8 pathway is activated in the *Eng*^{-/-} cells, because this pathway has been proposed to promote endothelial cell proliferation (7, 47).

TGF β is well known for regulating endothelial cell proliferation, extracellular matrix production in the vessel wall, vascular remodeling, and interactions between endothelium and vascular smooth muscle cells, along with their recruitment, and thus it has multiple roles in vascular development and maintenance of vessel integrity. Endothelial cells are unique in that they possess two type I receptor pathways activated by TGF β , the canonical ALK5 pathway, which activates Smad2/3, and the ALK1 pathway, which stimulates Smad1/5/8, a bone

morphogenetic protein-like pathway. Furthermore, Goumans *et al.* (46) have shown that ALK5 is important for recruitment of ALK1 into a TGF β receptor complex and that ALK5 kinase activity is essential for efficient ALK1 activation. Thus TGF β can activate the Smad1/5/8 pathway in endothelial cells via a composite type I receptor.

Endoglin is also expressed at high levels in endothelial cells and can associate with TGF β receptor complexes. Moreover, because mutations in *ENG* and *ACVRL1* both lead to HHT, it is intriguing to speculate that endoglin is required for the function of the composite ALK5-ALK1 receptor. Indeed, Lebrin *et al.* (7) recently reported that small interfering RNA-mediated knockdown of endoglin in MEEC resulted in loss of TGF β -dependent Smad1 activation and reduced proliferation of the cells. This led to the suggestion that endoglin is required for TGF β -dependent activation of ALK1 and subsequent Smad1/5/8 signaling. Our results stand in stark contrast. Using two MEEC lines that are null for *Eng*, we observed that both lines displayed enhanced proliferation and more robust activation of the Smad1/5/8 pathway in response to TGF β with little effect on Smad2/3 activation. Thus, we have unambiguously demonstrated that endoglin is not required for TGF β -dependent activation of the Smad1/5/8 pathway in the vascular endothelium.

What is the basis for the differences in MEEC responsiveness upon loss of *Eng* that is reported in our study versus that of Lebrin *et al.* (7)? In our study we found that deletion of *Eng* led to up-regulation of ALK5, a reduction in T β R β II levels, and no change in ALK1 levels. At the cell surface this resulted in fewer TGF β binding sites but of higher affinity, and this translated into a more robust TGF β -dependent activation of Smad1/5/8. Thus we propose that in our *Eng*^{-/-} MEEC, increased ALK5 levels recruit more ALK1 into receptor complexes to promote Smad1 activation at lower doses of TGF β . However, Lebrin *et al.* (7) reported that knockdown of endoglin resulted in decreased ALK5 levels. As ALK1 function is exquisitely sensitive to the levels of ALK5, the differences between these two studies may simply reflect how the TGF β receptor system, and in particular ALK5 expression, responds to loss of endoglin achieved by small interfering RNA technology versus gene ablation. Altogether, these results show that endoglin is not required for TGF β -dependent activation of Smad1/5/8 *per se* and suggest an alternative model in which endoglin controls cell surface receptor levels and binding characteristics. Moreover, as endoglin associates with other Ser/Thr kinase receptors (17), it may play similar roles in other bone morphogenetic protein (BMP) pathways that are not easily dissected by simple stimulation of cells with saturating concentrations of BMP. It will be interesting to determine whether interaction of endoglin with TGF β signaling receptors directly regulates cell surface levels and binding characteristics or whether alternative endoglin signaling pathways are responsible for controlling receptor expression.

How TGF β receptor expression is altered by endoglin loss is thus key to determining the resultant impact on TGF β responsiveness and Smad pathway activation. This may vary with the cell type or the differentiation status and underlie specific defects during development and homeostasis. Furthermore, as ALK1 and endoglin null mice have similar phenotypes and the loss of one allele of either gene results in HHT, it has been attractive to conclude that endoglin acts with ALK1 in the same TGF β pathway. However, vascular development involves complex tissue interactions initiated with vasculogenesis, when the primary capillary plexus is formed. This is followed by angiogenesis, which involves endothelial cell proliferation, migration, and remodeling of the primary endothelial network into a mature circulatory system (48). During angiogenesis,

endothelial cells recruit mesenchymal cell progenitors; upon contact, latent TGF β is activated, which induces differentiation to pericytes or smooth muscle cells. A recent report by Carvalho *et al.* (49) indicates that the defect in yolk sac vasculature of *Eng* null mice may in fact reflect reduced availability of TGF β protein and impaired recruitment and differentiation of smooth muscle cells. Accordingly, addition of exogenous TGF β 1 to yolk sac cells overcame the defect, confirming that it was the reduced production of TGF β 1 by the endothelium that was responsible for the apparent inability of mesenchymal cells to differentiate normally. Consistent with this, endothelial cells from HHT1 patients secrete less TGF β 1 and have lower plasma levels than do controls (50). Thus, defining how the loss of endoglin affects cell responsiveness versus TGF β 1 levels or access *in vivo* will help define how it impairs vascular development and homeostasis.

Acknowledgments—We thank Drs. C. LeRoy and M. Toporsian for helpful discussions.

REFERENCES

- Gougos, A., and Letarte, M. (1990) *J. Biol. Chem.* **265**, 8361–8364
- Burrows, F. J., Derbyshire, E. J., Tazzari, P. L., Amlot, P., Gazzdar, A. F., King, S. W., Letarte, M., Vitetta, E. S., and Thorpe, P. E. (1995) *Clin. Cancer Res.* **1**, 1623–1634
- Bodey, B., Bodey, B., Jr., Siegel, S. E., and Kaiser, H. E. (1998) *Anticancer Res.* **18**, 1485–1500
- Miller, D. W., Graulich, W., Karges, B., Stahl, S., Ernst, M., Ramaswamy, A., Sedlacek, H. H., Muller, R., and Adamkiewicz, J. (1999) *Int. J. Cancer* **81**, 568–572
- Duff, S. E., Li, C., Garland, J. M., and Kumar, S. (2003) *FASEB J.* **17**, 984–992
- Fonsatti, E., Altomonte, M., Arslan, P., and Maio, M. (2003) *Curr. Drug Targets* **4**, 291–296
- Lebrin, F., Goumans, M. J., Jonker, L., Carvalho, R. L., Valdimarsdottir, G., Thorikay, M., Mummery, C., Arthur, H. M., and ten Dijke, P. (2004) *EMBO J.* **23**, 4018–4028
- Conley, B. A., Smith, J. D., Guerrero-Esteo, M., Bernabeu, C., and Vary, C. P. (2000) *Atherosclerosis* **153**, 323–335
- Ma, X., Labinaz, M., Goldstein, J., Miller, H., Keon, W. J., Letarte, M., and O'Brien, E. (2000) *Arterioscler. Thromb. Vasc. Biol.* **20**, 2546–2552
- Adam, P. J., Clesham, G. J., and Weissberg, P. L. (1998) *Biochem. Biophys. Res. Commun.* **247**, 33–37
- Bourdeau, A., Dumont, D. J., and Letarte, M. (1999) *J. Clin. Investig.* **104**, 1343–1351
- Li, D. Y., Sorensen, L. K., Brooke, B. S., Urness, L. D., Davis, E. C., Taylor, D. G., Boak, B. B., and Wendel, D. P. (1999) *Science* **284**, 1534–1537
- Arthur, H. M., Ure, J., Smith, A. J., Renforth, G., Wilson, D. I., Torsney, E., Charlton, R., Parums, D. V., Jowett, T., Marchuk, D. A., Burn, J., and Diamond, A. G. (2000) *Dev. Biol.* **217**, 42–53
- Qu, R., Silver, M. M., and Letarte, M. (1998) *Cell Tissue Res.* **292**, 333–343
- McAllister, K. A., Grogg, K. M., Johnson, D. W., Gallione, C. J., Baldwin, M. A., Jackson, C. E., Helmbold, E. A., Markel, D. S., McKinnon, W. C., Murrell, J., McCormick, M. K., Pericak-Vance, M. A., Heutink, P., Oostra, B. A., Haitjema, T., Westerman, C. J. J., Porteus, M. E., Guttmacher, A. E., Letarte, M., and Marchuk, D. A. (1994) *Nat. Genet.* **8**, 345–351
- Pece, N., Vera, S., Cymerman, U., White, R. I., Jr., Wrana, J. L., and Letarte, M. (1997) *J. Clin. Investig.* **100**, 2568–2579
- Barbara, N. P., Wrana, J. L., and Letarte, M. (1999) *J. Biol. Chem.* **274**, 584–594
- Massague, J. (1998) *Annu. Rev. Biochem.* **67**, 753–791
- Roberts, A. B. (1999) *Microbes Infect.* **1**, 1265–1273
- Wrana, J. L., Attisano, L., Carcamo, J., Zentella, A., Doody, J., Laiho, M., Wang, X. F., and Massague, J. (1992) *Cell* **71**, 1003–1014
- Wrana, J. L., Attisano, L., Wieser, R., Ventura, F., and Massague, J. (1994) *Nature* **370**, 341–347
- Attisano, L., and Wrana, J. L. (2002) *Science* **296**, 1646–1647
- Chen, Y. G., and Massague, J. (1999) *J. Biol. Chem.* **274**, 3672–3677
- Oh, S. P., Seki, T., Goss, K. A., Imamura, T., Yi, Y., Donahoe, P. K., Li, L., Miyazono, K., ten Dijke, P., Kim, S., and Li, E. (2000) *Proc. Natl. Acad. Sci. U. S. A.* **97**, 2626–2631
- Shi, Y., and Massague, J. (2003) *Cell* **113**, 685–700
- Hayashi, H., Abdollah, S., Qiu, Y., Cai, J., Xu, Y. Y., Grinnell, B. W., Richardson, M. A., Topper, J. N., Gimbrone, M. A., Jr., Wrana, J. L., and Falb, D. (1997) *Cell* **89**, 1165–1173
- Kavak, P., Rasmussen, R. K., Causing, C. G., Bonni, S., Zhu, H., Thomsen, G. H., and Wrana, J. L. (2000) *Mol. Cell* **6**, 1365–1375
- Di Guglielmo, G. M., Le Roy, C., Goodfellow, A. F., and Wrana, J. L. (2003) *Nat. Cell Biol.* **5**, 410–421
- Pepper, M. S. (1997) *Cytokine Growth Factor Rev.* **8**, 21–43
- Hirschi, K. K., Rohovsky, S. A., and D'Amore, P. A. (1998) *J. Cell Biol.* **141**, 805–814
- Lebrin, F., Deckers, M., Bertolino, P., and Ten Dijke, P. (2005) *Cardiovasc. Res.* **65**, 599–608
- Johnson, D. W., Berg, J. N., Baldwin, M. A., Gallione, C. J., Marondel, I., Yoon, S. J., Stenzel, T. T., Speer, M., Pericak-Vance, M. A., Diamond, A., Guttmacher, A. E., Jackson, C. E., Attisano, L., Kucherlapati, R., Porteus,

- M. E., and Marchuk, D. A. (1996) *Nat. Genet.* **13**, 189–195
33. Abdalla, S. A., Pece-Barbara, N., Vera, S., Tapia, E., Paez, E., Bernabeu, C., and Letarte, M. (2000) *Hum. Mol. Genet.* **9**, 1227–1237
34. Guerrero-Esteo, M., Sanchez-Elsner, T., Letamendia, A., and Bernabeu, C. (2002) *J. Biol. Chem.* **277**, 29197–29209
35. Lastres, P., Letamendia, A., Zhang, H., Rius, C., Almendro, N., Raab, U., Lopez, L. A., Langa, C., Fabra, A., Letarte, M., and Bernabeu, C. (1996) *J. Cell Biol.* **133**, 1109–1121
36. Letamendia, A., Lastres, P., Botella, L. M., Raab, U., Langa, C., Velasco, B., Attisano, L., and Bernabeu, C. (1998) *J. Biol. Chem.* **273**, 33011–33019
37. Li, C., Hampson, I. N., Hampson, L., Kumar, P., Bernabeu, C., and Kumar, S. (2000) *FASEB J.* **14**, 55–64
38. Balconi, G., Spagnuolo, R., and Dejana, E. (2000) *Arterioscler. Thromb. Vasc. Biol.* **20**, 1443–1451
39. Attisano, L., Wrana, J. L., Cheifetz, S., and Massague, J. (1992) *Cell* **68**, 97–108
40. Massague, J. (1985) *Prog. Med. Virol.* **32**, 142–158
41. Muller, G., Behrens, J., Nussbaumer, U., Bohlen, P., and Birchmeier, W. (1987) *Proc. Natl. Acad. Sci. U. S. A.* **84**, 5600–5604
42. Roberts, A. B., and Sporn, M. B. (1989) *Am. Rev. Respir. Dis.* **140**, 1126–1128
43. Partridge, E. A., Le Roy, C., Di Guglielmo, G. M., Pawling, J., Cheung, P., Granovsky, M., Nabi, I. R., Wrana, J. L., and Dennis, J. W. (2004) *Science* **306**, 120–124
44. Ota, T., Fujii, M., Sugizaki, T., Ishii, M., Miyazawa, K., Aburatani, H., and Miyazono, K. (2002) *J. Cell Physiol.* **193**, 299–318
45. Macias-Silva, M., Hoodless, P. A., Tang, S. J., Buchwald, M., and Wrana, J. L. (1998) *J. Biol. Chem.* **273**, 25628–25636
46. Goumans, M. J., Valdimarsdottir, G., Itoh, S., Lebrin, F., Larsson, J., Mummery, C., Karlsson, S., and ten Dijke, P. (2003) *Mol. Cell* **12**, 817–828
47. Goumans, M. J., Valdimarsdottir, G., Itoh, S., Rosendahl, A., Sideras, P., and ten Dijke, P. (2002) *EMBO J.* **21**, 1743–1753
48. Folkman, J., and D'Amore, P. A. (1996) *Cell* **87**, 1153–1155
49. Carvalho, R. L., Jonker, L., Goumans, M. J., Larsson, J., Bouwman, P., Karlsson, S., Dijke, P. T., Arthur, H. M., and Mummery, C. L. (2004) *Development* **131**, 6237–6247
50. Letarte, M., McDonald, M. L., Li, C., Kathirkamathamby, K., Vera, S., Pece-Barbara, N., and Kumar, S. (2005) *Cardiovas. Res.* in press

Endoglin Null Endothelial Cells Proliferate Faster and Are More Responsive to Transforming Growth Factor β 1 with Higher Affinity Receptors and an Activated Alk1 Pathway

Nadia Pece-Barbara, Sonia Vera, Kirishanthy Kathirkamathamby, Stefan Liebner, Gianni M. Di Guglielmo, Elisabetta Dejana, Jeffrey L. Wrana and Michelle Letarte

J. Biol. Chem. 2005, 280:27800-27808.

doi: 10.1074/jbc.M503471200 originally published online May 27, 2005

Access the most updated version of this article at doi: [10.1074/jbc.M503471200](https://doi.org/10.1074/jbc.M503471200)

Alerts:

- [When this article is cited](#)
- [When a correction for this article is posted](#)

[Click here](#) to choose from all of JBC's e-mail alerts

This article cites 49 references, 19 of which can be accessed free at <http://www.jbc.org/content/280/30/27800.full.html#ref-list-1>